

## $\gamma$ -RAY SPECTRAL EVOLUTION OF NGC 1275 OBSERVED WITH *FERMI* LARGE AREA TELESCOPE

J. KATAOKA<sup>1</sup>, Ł. STAWARZ<sup>2,3</sup>, C. C. CHEUNG<sup>4</sup>, G. TOSTI<sup>5,6</sup>, E. CAVAZZUTI<sup>7</sup>, A. CELOTTI<sup>8</sup>, S. NISHINO<sup>9</sup>, Y. FUKAZAWA<sup>9</sup>,  
D. J. THOMPSON<sup>10</sup>, AND W. F. MC CONVILLE<sup>10,11</sup>

<sup>1</sup> Research Institute for Science and Engineering, Waseda University, 3-4-1, Okubo, Shinjuku, Tokyo 169-8555, Japan

<sup>2</sup> Institute of Space and Astronautical Science, JAXA, 3-1-1, Yoshinodai, Sagamihara, Kanagawa 252-5210, Japan

<sup>3</sup> Astronomical Observatory, Jagiellonian University, ul. Orla 171, Kraków 30-244, Poland

<sup>4</sup> NRC Research Associate, Space Science Division, Naval Research Laboratory, Washington, DC 20375, USA

<sup>5</sup> Istituto Nazionale di Fisica Nucleare, Sezione di Perugia, I-06123 Perugia, Italy

<sup>6</sup> Dipartimento di Fisica, Università degli Studi di Perugia, I-06123 Perugia, Italy

<sup>7</sup> Agenzia Spaziale Italiana (ASI) Science Data Center, I-00044 Frascati (Roma), Italy

<sup>8</sup> Scuola Internazionale Superiore di Studi Avanzati (SISSA), 34014 Trieste, Italy

<sup>9</sup> Department of Physical Sciences, Hiroshima University, Higashi-Hiroshima, Hiroshima 739-8526, Japan

<sup>10</sup> NASA Goddard Space Flight Center, Greenbelt, MD 20771, USA

<sup>11</sup> Department of Physics, University of Maryland, College Park, MD 20742, USA

Received 2010 March 10; accepted 2010 April 10; published 2010 April 29

### ABSTRACT

We report on a detailed investigation of the high-energy  $\gamma$ -ray emission from NGC 1275, a well-known radio galaxy hosted by a giant elliptical located at the center of the nearby Perseus cluster. With the increased photon statistics, the center of the  $\gamma$ -ray-emitting region is now measured to be separated by only 0.46 arcmin from the nucleus of NGC 1275, well within the 95% confidence error circle with radius  $\simeq 1.5$  arcmin. Early *Fermi* Large Area Telescope (LAT) observations revealed a significant decade-timescale brightening of NGC 1275 at GeV photon energies, with a flux about 7 times higher than the one implied by the upper limit from previous EGRET observations. With the accumulation of one year of *Fermi*-LAT all-sky-survey exposure, we now detect flux and spectral variations of this source on month timescales, as reported in this paper. The average  $>100$  MeV  $\gamma$ -ray spectrum of NGC 1275 shows a possible deviation from a simple power-law shape, indicating a spectral cutoff around an observed photon energy of  $\varepsilon_\gamma = 42.2 \pm 19.6$  GeV, with an average flux of  $F_\gamma = (2.31 \pm 0.13) \times 10^{-7}$  photons cm $^{-2}$  s $^{-1}$  and a power-law photon index,  $\Gamma_\gamma = 2.13 \pm 0.02$ . The largest  $\gamma$ -ray flaring event was observed in 2009 April–May and was accompanied by significant spectral variability above  $\varepsilon_\gamma \gtrsim 1\text{--}2$  GeV. The  $\gamma$ -ray activity of NGC 1275 during this flare can be described by a hysteresis behavior in the flux versus photon index plane. The highest energy photon associated with the  $\gamma$ -ray source was detected at the very end of the observation, with the observed energy of  $\varepsilon_\gamma = 67.4$  GeV and an angular separation of about 2.4 arcmin from the nucleus. In this paper we present the details of the *Fermi*-LAT data analysis, and briefly discuss the implications of the observed  $\gamma$ -ray spectral evolution of NGC 1275 in the context of  $\gamma$ -ray blazar sources in general.

**Key words:** galaxies: active – galaxies: individual (NGC 1275) – galaxies: jets – gamma rays: general – radiation mechanisms: non-thermal

### 1. INTRODUCTION

With the successful launch of the *Fermi Gamma-ray Space Telescope*, we have a new opportunity to study the  $\gamma$ -ray emission from different types of extragalactic sources—not only blazars, but also radio galaxies and possibly other classes of active galactic nuclei (AGNs)—with much improved sensitivity than previously available (Abdo et al. 2010a). During the initial all-sky survey performed during the first 4 months after its launch, the *Fermi* Large Area Telescope (LAT) detected only two radio galaxies at high significance ( $\geq 10\sigma$ ), namely, NGC 1275 (Abdo et al. 2009a; hereafter Paper I) and Cen A (Abdo et al. 2009b, 2009c). More recently, the detection of MeV/GeV emission from yet another famous radio galaxy M 87, an established TeV source, was reported based on 10 months of all-sky-survey *Fermi*-LAT data (Abdo et al. 2009d). Yet the detection of NGC 1275 was particularly noteworthy because this source, unlike Cen A or M 87, was previously undetected in  $\gamma$ -rays, neither by *CGRO*/EGRET during its  $\sim 10$  years of operation, nor by ground-based Cherenkov telescopes. The  $\gamma$ -ray flux of NGC 1275 detected by the *Fermi*-LAT was about seven times higher than the one implied by the  $2\sigma$  upper limit reported by EGRET, namely,  $F_{\varepsilon_\gamma > 100 \text{ MeV}} <$

$3.72 \times 10^{-8}$  photons cm $^{-2}$  s $^{-1}$  (Reimer et al. 2003). We note that *COS B* data taken between 1975 and 1979 (Strong et al. 1982; Mayer-Hasselwander et al. 1982) showed a  $\gamma$ -ray excess coincident with the position of this galaxy, although the evidence for the claimed high-energy source to be *uniquely* related to NGC 1275 is ambiguous.

NGC 1275 is a giant elliptical galaxy located at the center of the Perseus cluster.<sup>12</sup> This cluster is the brightest cluster of galaxies in the X-ray band (e.g., Böhringer et al. 1993; Fabian et al. 2003, 2006), and as such it has been the focus of several extensive research programs over many years and across the entire available electromagnetic spectrum. When observed at radio wavelengths, NGC 1275 hosts the exceptionally bright radio FR I radio galaxy Perseus A = 3C 84 (e.g., Vermeulen et al. 1994; Taylor & Vermeulen 1996; Walker et al. 2000; Asada et al. 2006). Although high-energy  $\gamma$ -rays may in general be produced within the intergalactic/interstellar medium of the Perseus cluster, in Paper I, we argued that the inner radio jet of 3C 84 was the most likely source of the observed  $\gamma$ -ray

<sup>12</sup> The Perseus cluster (Abell 426): redshift  $z = 0.0179$ , luminosity distance  $d_L = 75.3$  Mpc, scale  $21.5$  kpc arcmin $^{-1}$  (for flat cosmology with  $H_0 = 71$  km s $^{-1}$  Mpc $^{-1}$  and  $\Omega_M = 0.27$ ).

photons because of the variability of the MeV/GeV flux on year/decade timescales implied by the EGRET and early *Fermi*-LAT observations. Specifically, these measurements implied the  $\gamma$ -ray emission region size in NGC 1275 has a radius,  $R \lesssim ct_{\text{var}} \simeq 1$  pc. Note, however, that no significant variability was detected within the 4 month long *Fermi*-LAT data set analyzed in Paper I. Also, the LAT error circle determined from these initial data was too large to exclude possible contributions from other galaxies to the observed  $\gamma$ -ray flux (specifically, NGC 1273, 1274, 1277, 1278, and 1279 were still within the previously determined 95% error circle with  $R = 5.2$  arcmin).

Meanwhile, follow-up observations by the VERITAS Cherenkov telescope (Weekes et al. 2002) put strong constraints on the very high-energy (VHE)  $\gamma$ -ray emission from NGC 1275 above 100 GeV. In particular, no VHE  $\gamma$ -ray emission from NGC 1275 was detected by VERITAS, with a 99% confidence level upper limit of 2.1% of the Crab Nebula flux, corresponding to 19% of the power-law extrapolation of the MeV/GeV flux observed during the first 4 months of the *Fermi*-LAT observations (assuming the photon index,  $\Gamma_\gamma \simeq 2.2$ ; Acciari et al. 2009b). This naturally indicates a deviation from the pure power-law spectrum in the VHE regime, possibly compatible with the presence of an exponential cutoff around or below photon energies  $\varepsilon_\gamma \simeq 100$  GeV (Acciari et al. 2009b). The MAGIC Cherenkov telescope also recently measured upper limits for the VHE  $\gamma$ -ray emission of NGC 1275, namely,  $F_{\varepsilon_\gamma > 100 \text{ GeV}} < (4.6\text{--}7.5) \times 10^{-12}$  photons  $\text{cm}^{-2} \text{s}^{-1}$  for the photon indices ranging from 1.5 up to 2.5 (Aleksić et al. 2010). Thus, the implied deviation in the  $\gamma$ -ray spectrum of 3C 84 from a simple power-law form, as well as a possibility for a short-timescale (< month) variability of the Perseus A  $\gamma$ -ray flux, may now be finally addressed and re-examined by *Fermi*-LAT, due to the much improved photon statistic (especially above 10 GeV) after the one-year-all-sky survey. Obviously, such deep studies of NGC 1275 in the MeV/GeV photon energy range are of major importance for understanding the whole class of  $\gamma$ -ray-emitting radio galaxies in general.

Firmly motivated, we performed a detailed investigation of NGC 1275 in  $\gamma$ -rays based on the accumulation of one year of *Fermi*-LAT all-sky-survey data. In particular, we aimed to address the following problems: (1) presence of short-timescale  $\gamma$ -ray flux variability, (2) positional coincidence of the  $\gamma$ -ray-emitting center with the active nucleus of NGC 1275, and (3) spectral curvature and spectral evolution of NGC 1275 in the MeV/GeV photon energy range. In Section 2, we describe the *Fermi*-LAT  $\gamma$ -ray observations and data reduction procedure. The results of the analysis are given in Section 3, and the discussion and conclusions are presented in Section 4.

## 2. *Fermi*-LAT OBSERVATIONS

The LAT instrument on board *Fermi* is described in detail in Atwood et al. (2009), and references therein. Compared to earlier  $\gamma$ -ray missions, the LAT has a large effective area ( $\sim 8000 \text{ cm}^2$  on axis at 1 GeV for the event class considered here), wide energy coverage (from  $\approx 20$  MeV to  $> 300$  GeV), and improved angular resolution. The 68% containment angles of the reconstructed incoming photon direction are approximated as  $\theta_{68} \simeq 0^\circ.8 (\varepsilon_\gamma/\text{GeV})^{-0.8}$  below 10 GeV, giving  $\theta_{68} \sim 5^\circ.1$  at 100 MeV and  $\sim 0^\circ.15$  at 10 GeV (update of values presented in Atwood et al. 2009). Above 10 GeV, the improvement of angular resolution becomes relatively gentle, such that  $\theta_{68} \sim 0^\circ.07$  at 100 GeV. During the first year of operations, most of the telescope's time was dedicated to observing in "survey

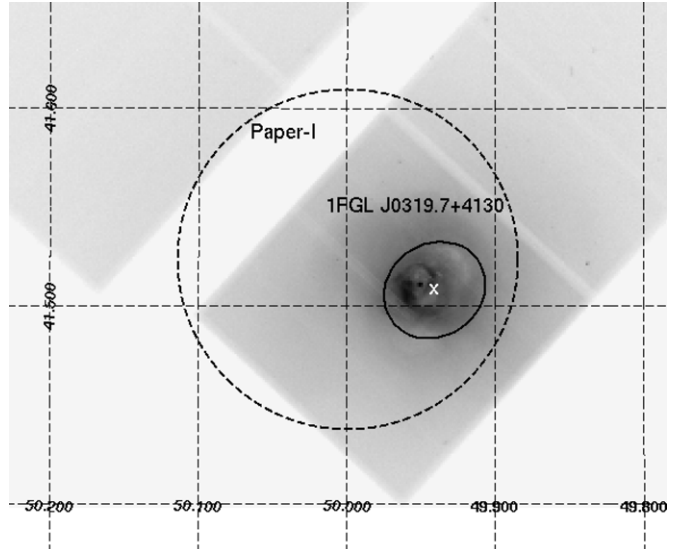


**Figure 1.** Ninety-five percent LAT  $\gamma$ -ray localization error circles placed on the *Chandra* ACIS-S image constructed between 0.4 and 8.0 keV. The positional center of the  $\gamma$ -ray emission, marked as the white "X," is only 0.46 arcmin from the position of the NGC 1275 nucleus, with 95% radii of  $r_{95} = 5.2$  arcmin for Paper I and 1.5 arcmin (more accurately,  $1.56 \times 1.38$  arcmin; Abdo et al. 2010b) for 11 months, respectively.

mode" where *Fermi* points away from the Earth and nominally rocks the spacecraft axis north and south from the orbital plane to enable monitoring of the entire sky on a timescale shorter than a day. The whole sky is surveyed every  $\sim 3$  hr (or two orbits). The total live time included is 280.3 days (24.21 Ms). This corresponds to an absolute efficiency of 75%. Most of the inefficiency is due to time lost during passages through the South Atlantic Anomaly and to readout dead time.

The observations used here comprises all scientific data obtained between 2008 August 4 and 2009 August 13. This time interval runs from Mission Elapsed Time (MET) 239557417 to 271844550. We have applied the zenith angle cut of  $105^\circ$  to eliminate photons from Earth's limb. The same zenith cut is also accounted for in the exposure calculation using the LAT science tool<sup>13</sup> GTLCUBE. We use the "Diffuse" class events (Atwood et al. 2009), which are those reconstructed events having the highest probability of being photons. In the analysis presented here, we set the lower energy bound to a value of 100 MeV. Science Tools version v9r15p2 and Instrumental Response Functions (IRFs) P6\_V3 (a model of the spatial distribution of photon events calibrated post-launch) were used throughout this paper. The early portion of the data here coincides with the early LAT observations of NGC 1275 presented in Paper I (2008 August 4 and 2008 December 5).

## 2.1. Results

Figure 1 shows the LAT 95%  $\gamma$ -ray localization error circles placed on the *Chandra* ACIS-S X-ray image of NGC 1275/Perseus region (ObsID 4952; exposure 164 ks). The *Chandra* image is constructed between 0.4 and 8.0 keV. The positional center of the  $\gamma$ -ray emission (R.A. =  $49^\circ 941$ , decl. =  $41^\circ 509$ ) is taken from the 11 month catalog (1FGL J0319.7+4130; Abdo et al. 2010b), and is only 0.46 arcmin from the NGC 1275 nucleus (R.A. =  $49^\circ 951$ , decl. =  $41^\circ 512$ ),

<sup>13</sup> <http://fermi.gsfc.nasa.gov/ssc/data/analysis/documentation/Cicerone/>

with 95% radius  $\simeq 1.5$  arcmin (Figure 1). Since the localization error has been substantially improved compared to the one quoted in Paper I (5.2 arcmin, based on the 3 month bright source list; Abdo et al. 2009c), all the other field galaxies mentioned in Paper I within the 3 month LAT error (NGC 1273, 1274, 1277, 1278, and 1279) are now outside the 11 month LAT error circle. Indeed, even the nearest galaxy, NGC 1274, is 2.6 arcmin apart from the positional center of the  $\gamma$ -ray emission with 95% radius of 1.5 arcmin. With the good positional association described above, we thus believe the  $\gamma$ -ray source is most likely identified as the nucleus of NGC 1275, but still needing further confirmation based on correlated variability with observations at other wavelengths.

We also checked the projection of the  $\gamma$ -ray images as presented in Paper I. The counts distributions of NGC 1275 in different energy bands are consistent with the distributions for a point source, indicating that the diffuse extended component does not contaminate the NGC 1275/Perseus  $\gamma$ -ray source, even with much improved photon statistics in the one-year data set. Since the angular resolution of the LAT improves at high energies (Atwood et al. 2009, and see above), it is interesting to compare the reconstructed incoming photon directions with the position of the NGC 1275 nucleus around the higher energy photons that can be detected with the *Fermi*-LAT. Figure 2 shows the angular separation of  $\varepsilon_\gamma > 10$  GeV photons from the nucleus of NGC 1275 as a function of photon energy. The 68% and 95% angular resolutions of *Fermi*-LAT are shown as dotted and dashed lines, respectively. The angular displacement of the highest energy photon detected during one-year-all-sky survey ( $\varepsilon_\gamma \simeq 67.4$  GeV; a double circle with a number “I” in Figure 2) from the nucleus is only 2.4 arcmin, which is well within the point-spread function (PSF) of the LAT at this energy ( $\theta_{68} \simeq 4.4$  arcmin). Note that the chance probability for detecting Galactic and/or extragalactic  $\gamma$ -ray background photons with energies at least 67.4 GeV within  $\theta_{68}$  is less than 0.1%; hence, we conclude that NGC 1275 is the most likely source of the discussed photon. The other three highest energy photons ( $\varepsilon_\gamma > 30$  GeV) are marked in Figure 2 as “II,” “III,” and “IV,” and are all well within the 95% PSF of the *Fermi*-LAT.

## 2.2. Spectral Analysis

To study the average spectrum of NGC 1275 during the one-year observation, we use the standard maximum-likelihood spectral estimator provided with the LAT science tools GTLIKE. This fits the data to a source model, along with the models for the uniform extragalactic and structured Galactic backgrounds.<sup>14</sup> We use a recent Galactic diffuse model, gll\_iem\_v02.fit, with the normalization free to vary in the fit. The response function used is P6\_V3\_DIFFUSE. Careful choice of the source region is important especially for relatively faint sources. Following the detailed study of changing the region of interest (ROI) radius from  $5^\circ$  to  $20^\circ$  in Paper I, we set  $r = 8^\circ$  in the following analysis to minimize the contamination from the Galactic diffuse emission. Only one point source, corresponding to src\_A in Paper I, was found in the ROI. The coordinates are R.A. =  $55^\circ 105$ , decl. =  $41^\circ 515$ , with  $r_{95} = 4.1$  arcmin. We modeled the source for subsequent spectral analysis (also see the *Fermi*-LAT bright  $\gamma$ -ray source list; Abdo et al. 2009c).

We first model the continuum  $\gamma$ -ray emission of NGC 1275 with a single power law. The extragalactic background is assumed to have a power-law spectrum as well, with the spectral

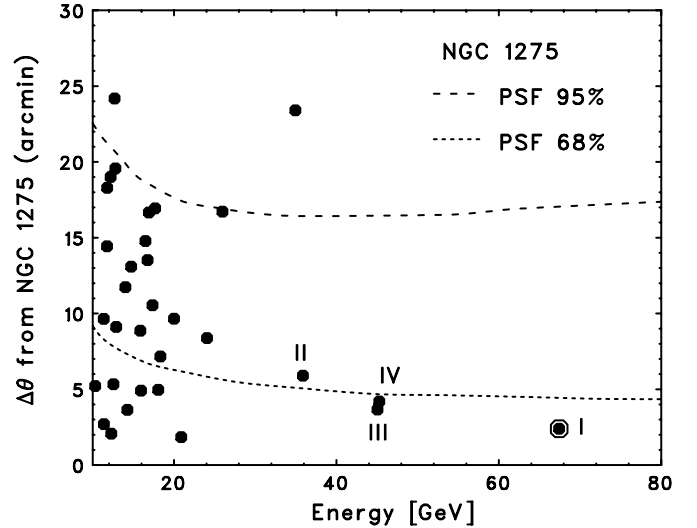


**Figure 2.** Angular separation of high-energy ( $\varepsilon_\gamma > 10$  GeV) photons from the nucleus of NGC 1275 as a function of photon energy. The 68% and 95% angular resolutions of *Fermi*-LAT are shown as dotted and dashed lines, respectively. These PSF profiles are derived for P6\_V3\_Diffuse and have been averaged over the acceptance of the LAT. The highest energy photon detected during the one-year-all-sky survey is  $\varepsilon_\gamma = 67.4$  GeV (double circle denoted as “I”), whose angular separation from NGC 1275 is only 2.4 arcmin. Arrival times of the four highest energy photons (“I–IV”) are indicated in Figure 4.

index and the normalization free to vary in the fit. From an unbinned GTLIKE analysis, the best-fit power-law parameters for NGC 1275 are

$$\frac{dN}{d\varepsilon_\gamma} = (2.61 \pm 0.14) \times 10^{-9} \left( \frac{\varepsilon_\gamma}{100 \text{ MeV}} \right)^{-2.13 \pm 0.02} \text{ photons cm}^{-2} \text{ s}^{-1} \text{ MeV}^{-1}, \quad (1)$$

or

$$F_{\varepsilon_\gamma > 100 \text{ MeV}} = (2.31 \pm 0.13) \times 10^{-7} \text{ photons cm}^{-2} \text{ s}^{-1}, \quad (2)$$

with only statistical errors taken into account. Systematic errors for the LAT are still under investigation, but the estimated systematic uncertainty on the flux is 10% at 100 MeV, 5% at 500 MeV, and 20% at 10 GeV, respectively (Abdo et al. 2010b). The results are consistent with those presented in Paper I, even though the uncertainties are now much smaller due to the improved photon statistics.

The predicted photon counts from NGC 1275 in the ROI are  $N_{\text{pred}} = 3187$  and the test statistic (defined as  $\text{TS} = 2[\log L - \log L_0]$ , where  $L$  and  $L_0$  are the likelihood when the source is included or not, respectively) is  $\text{TS} = 4039.8$  above  $\varepsilon_\gamma = 100$  MeV, corresponding to a  $64\sigma$  detection. For the Galactic diffuse background, the normalization is  $1.11 \pm 0.01$  and  $N_{\text{pred}} = 44835.3$ . The power-law photon index of the extragalactic background is  $\Gamma_\gamma = 2.31 \pm 0.03$  with  $N_{\text{pred}} = 9081.7$ . Figure 3 shows the LAT spectrum of NGC 1275 obtained by separately running GTLIKE for 10 energy bands; 100–200 MeV, 200–400 MeV, 400–800 MeV, 800 MeV–1.6 GeV, 1.6–3.2 GeV, 3.2–6.4 GeV, 6.4–12.8 GeV, 12.8–25.6 GeV, 25.6–51.2 GeV, and 51.2–102.4 GeV, where the dashed line shows the best-fit power-law function for the NGC 1275 data given in Equation (1). For the highest energy bin (51.2–102.4 GeV), we plot a  $2\sigma$  upper limit since this bin includes only one photon (see Figure 2) and is ignored in the subsequent statistical analysis.

<sup>14</sup> <http://fermi.gsfc.nasa.gov/ssc/data/access/lat/BackgroundModels.html>

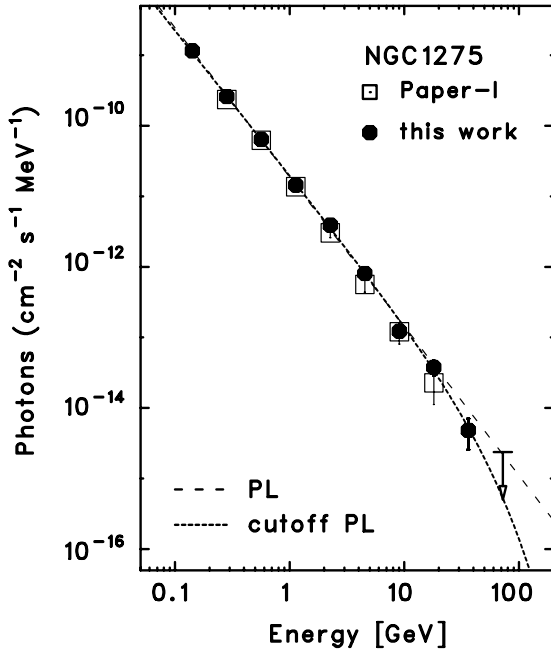


**Figure 3.** Average LAT > 100 MeV spectrum of NGC 1275 derived from one-year accumulation of data (filled circles; this work), as compared with that determined from the initial 4 month data set (open squares; Paper I). The dashed line shows the power-law function for the one-year data determined from the GTLIKE. The dotted line represents the best-fit cutoff power law with  $\epsilon_c = 42.2$  GeV as described in the text.

Note an indication of a deviation of the model with respect to the data above  $\epsilon_\gamma = 20$  GeV. Indeed, a  $\chi^2$  fit of the power-law model to the data<sup>15</sup> gives a relatively poor fit with  $\chi^2 = 14$  for 7 degrees of freedom (dof), where its probability is  $P(\chi^2) = 0.05$ . Instead, an alternative fit with a cutoff power-law function with the form  $dN/d\epsilon_\gamma \propto \epsilon_\gamma^{-\Gamma_\gamma} \times \exp[-\epsilon_\gamma/\epsilon_c]$  gives a much better representation of the data with an improved  $\chi^2 = 6.7$  for 7 dof, corresponding to  $P(\chi^2) = 0.34$ . We therefore retried the GTLIKE fit assuming a power law with an exponential cutoff function, and obtained  $\epsilon_c = 42.2 \pm 19.6$  GeV with  $\Gamma_\gamma = 2.07 \pm 0.03$ . Moreover, we apply a likelihood ratio test between a simple power-law and a cutoff power-law function. The test statistic ( $D$ ) is twice the difference in these log-likelihoods, which gives  $D = 2.9$  for our case. Note that the probability distribution of the test statistic can be approximated by a  $\chi^2$  distribution with 1 dof, corresponding to different degrees of freedom between two functions. We obtain  $P(\chi^2) \leq 0.08$ , which again indicates a deviation from a simple power-law function although this is currently inconclusive. The best-fit cutoff power-law function is shown as a dotted line in Figure 3.

### 2.3. Temporal Variability

Next, we investigated the  $\gamma$ -ray flux variations of NGC 1275 from 2008 August 4 to 2009 August 13. To this end, we constructed spectra with a time resolution of 14 days and fit each spectrum with a power-law model just for simplicity. The ROI radius ( $r = 8^\circ$ ), the energy range ( $\epsilon_\gamma > 100$  MeV), and other screening conditions are the same as described above. Since no variability is expected for the underlying background

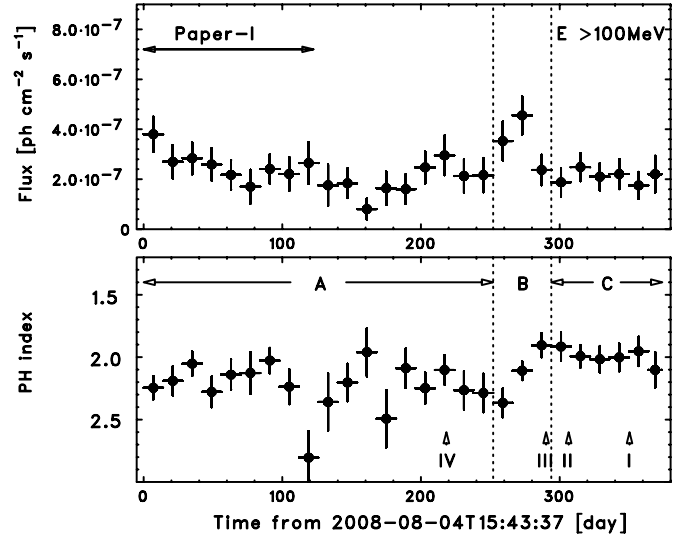


**Figure 4.** Temporal variation of  $\gamma$ -ray flux and spectral index over the period 2008 August–2009 August. The time (in days) is measured from the start of the *Fermi* observation, i.e., 2008 August 4, 15:43:37 UT. Upper panel: changes in the  $\epsilon_\gamma > 100$  MeV flux. Lower panel: changes in the power-law photon index. We have divided the analyzed time window into epochs A (before the flare), B (during the flare), and C (after the flare). The arrival times of the highest energy photons I–IV (Figure 2) are indicated as arrows. Background diffuse emission (both Galactic and extra-galactic) is fixed at the best-fit parameters determined from an average spectral fit as given in the text, and only statistical errors are shown.

diffuse emission, we fix the best-fit parameters to the average values determined from the one-year integrated spectrum for the Galactic and extragalactic background components. We first fix the spectral index to the best-fit value over the full interval,  $\Gamma_\gamma = 2.13$ , to minimize uncertainties in the flux estimates. In this case, variability is highly significant with  $\chi^2 = 157.7$  for 26 dof, where  $P(\chi^2) < 10^{-6}$ . Indeed, the  $\gamma$ -ray flux varies even within a few month timescale. Due to the limited photon statistics, however, it is difficult to investigate any shorter timescale variability of NGC 1275. We also investigate the spectral evolution of NGC 1275, with the  $\gamma$ -ray photon index free to vary. Figure 4 shows variations of the flux ( $\epsilon_\gamma > 100$  MeV: upper panel) and photon index (lower panel) versus time. A flaring event is seen around  $T = 252$ –294 days after 2008 August 4 (epoch “B” in Figure 4), corresponding to the epoch 2009 April–May. A doubling timescale for the flaring period cannot be accurately measured, but  $\sim 20$  days. A  $\chi^2$  fit to a constant gives 35.6 and 43.0 for 26 dof, corresponding to the probability  $P(\chi^2) = 0.10$  and 0.02, respectively, for the flux and the photon index variations. Interestingly, the spectral variation is predominantly due to the difference between the pre- and post-flare period, denoted in Figure 4 as epochs “A” and “C.” In fact, if we test the variability *separately* for the pre- and post-flare periods (A and C), the significance of the variability decreases substantially, such that a constant fit provides  $P(\chi^2) > 0.21$  or 0.29 for both the flux and the photon index changes. During the flare (epoch B), the photon index changes from  $\Gamma_\gamma \simeq 2.2$  to  $\Gamma_\gamma \leq 2.0$ . Note that, after the flare (epoch C), the flux drops to its original level but the spectrum remains relatively flat, with  $\Gamma_\gamma \simeq 2$ , persisting for more than a few months. It should also be noted that three out of the four highest energy photons (denoted as I, II, and III in Figure 2) were indeed detected in the post-flare period, when the spectrum appears the flattest.

<sup>15</sup> Note that the maximum likelihood itself does not provide any information about the quality of a fit for an assumed model. We therefore perform  $\chi^2$  fitting to the resultant 10 band LAT spectrum as described above, to give a convenient estimate of the goodness of the fit.

### 3. DISCUSSION AND CONCLUSION

In the previous sections, we reported on the analysis of the  $\gamma$ -ray emission from NGC 1275 observed with *Fermi*-LAT during its one-year-all-sky survey. We showed that with the increased photon statistics, the positional center of the  $\gamma$ -ray emission is now much closer to the NGC 1275 nucleus as compared to that reported in Paper I. In addition, we have shown that the average  $\gamma$ -ray spectrum of NGC 1275 reveals a significant deviation from a simple power law above photon energies  $\varepsilon_\gamma \sim 1\text{--}2$  GeV. That is, the observed *Fermi*-LAT spectrum is best fitted by a power-law function ( $\Gamma_\gamma \simeq 2.1$ ) with an exponential cutoff at the break photon energy  $\varepsilon_c = 42.2 \pm 19.6$  GeV. Finally, we argued that significant flux and spectral changes of NGC 1275 are detected with *Fermi*-LAT on a timescale of a few months, although the possibility for even shorter variability remains uncertain.

We also reported the detection of an interesting spectral evolution, consisting of a *persistent* (over more than a few months) spectral hardening (from  $\Gamma_\gamma \simeq 2.2$  to  $\Gamma_\gamma \simeq 2$ ) after the largest flaring event observed in 2009 April–May. During this flat-spectrum/low-flux-level epoch the highest energy photon ( $\varepsilon_\gamma \simeq 67.4$  GeV) was detected from the direction of NGC 1275. All these new findings basically support the idea put forward in Paper I that the observed  $\gamma$ -ray emission from the Perseus system originates in the (sub) pc-scale radio jet of NGC 1275, and is therefore most likely analogous to high-energy emission observed in blazars. In fact, as shown in Paper I, the overall  $\nu F_\nu$  spectral energy distribution (SED) of NGC 1275 constructed with multi-frequency radio to  $\gamma$ -ray data shows a close similarity to the “two-bump” SEDs of so-called low-frequency peaked BL Lac objects (hereafter LBLs). Till now, only a few LBLs have been detected at TeV photon energies—BL Lac (Albert et al. 2007), 3C 66A (Acciari et al. 2009a), S5 0716+714 (Anderhub et al. 2009), and also W Comae from an IBL class (Acciari et al. 2008; 2009d)—and more similar discoveries are expected. Hence, NGC 1275 itself has been suggested to be a potential TeV source as well, thus motivating deep VERITAS (Acciari et al. 2009b) and MAGIC (Aleksić et al. 2010) observations. These observations so far resulted only in upper limits to the VHE  $\gamma$ -ray emission of the studied region. One should note, however, that both the low- and high-energy peaks of NGC 1275 (in the  $\nu F_\nu$  representations) are located at substantially lower frequencies than those of typical LBLs. Indeed, the low-energy (synchrotron) emission components of 3C 66A and BL Lac peak around  $10^{13\text{--}15}$  Hz, while it is around  $10^{12}$  Hz in the case of NGC 1275 (Paper I). Correspondingly, the high-energy emission component of 3C 66A (but not necessarily of BL Lac) peaks at higher photon energies than that observed in NGC 1275. Within such an interpretation, this is consistent with the softer MeV/GeV spectrum in NGC 1275 ( $\Gamma_\gamma = 2.13 \pm 0.02$ ) compared to 3C 66A ( $\Gamma_\gamma = 1.97 \pm 0.04$ ; Abdo et al. 2009b) as measured by the *Fermi*-LAT. Note also that the X-ray spectrum of NGC 1275 is clearly “rising” in the  $\nu F_\nu$  representation ( $\Gamma_X = 1.6\text{--}1.7$ ; Balmaverde et al. 2006; Ajello et al. 2009), indicating that it is dominated by the low-energy portion of the inverse Compton (IC) emission, whilst the X-ray spectra of LBLs are typically very flat, suggesting a transition between the synchrotron and IC components ( $\Gamma_X \simeq 2$ ; e.g., Ghisellini et al. 1998). Such observational differences may indicate that, unlike in the case of LBLs, the high-energy spectrum of NGC 1275 does not extend up to TeV photon energies.

An interesting comparison can be made to another nearby radio galaxy detected by *Fermi*-LAT, namely, M 87 which re-

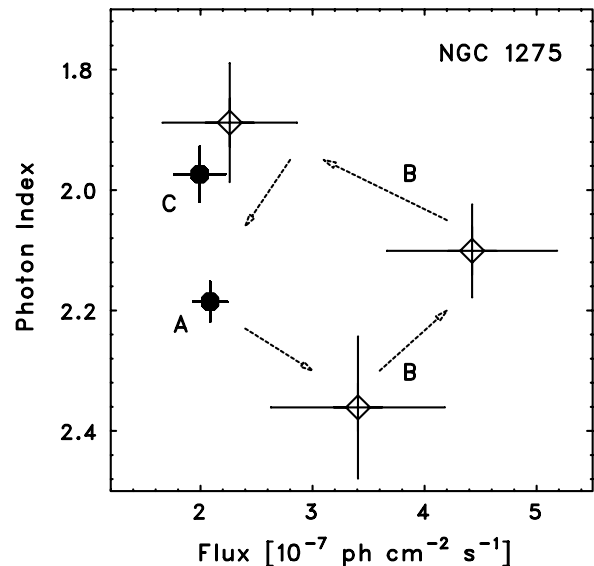


**Figure 5.** Spectral evolution of NGC 1275 in the flux–photon index representation. Labels “A” and “C” denote the average fluxes and photon indices determined for the period before (0–252 days) and after the flare (294–374 days), respectively (see Figure 4). Label “B” denotes the spectral evolution during the flare with a time bin of 2 weeks. Note that the photon index changes significantly before and after the flare, while the flux levels are comparable.

sembles NGC 1275 in many respects, and is an established TeV source (Abdo et al. 2009d). While M 87 is closer to us than NGC 1275 ( $d_L = 16$  Mpc versus  $d_L = 75.3$  Mpc), the GeV flux of M 87 is much lower than that of NGC 1275 ( $F_{\varepsilon_\gamma > 100 \text{ MeV}} = (2.45 \pm 0.63) \times 10^{-8} \text{ photons cm}^{-2} \text{ s}^{-1}$  versus  $(2.31 \pm 0.13) \times 10^{-7} \text{ photons cm}^{-2} \text{ s}^{-1}$ ), with similar LAT measured spectra ( $\Gamma_\gamma = 2.26 \pm 0.13$  versus  $2.13 \pm 0.02$ ). Note also that both radio galaxies are located at the centers of rich clusters, that the synchrotron emission components in both sources peak in the far infrared ( $\sim 10^{12}\text{--}10^{13}$  Hz), and the estimated jet powers are similar,  $L_j \sim 10^{44} \text{ erg s}^{-1}$  (Owen et al. 2000; Dunn & Fabian 2004). Thus, it may be surprising that only one of these has so far been detected at TeV photon energies. The detailed analysis of the spectral evolution of NGC 1275 within the *Fermi*-LAT range reported in this paper may provide a viable explanation for such a behavior. In particular, as already emphasized above, we found that the epochs characterized by the flattest GeV continuum of this source, as well as the arrival times of the highest energy photons from the direction of NGC 1275, do not coincide with the epochs of the highest photon flux above 100 MeV. This is clearly illustrated in Figure 5, which shows a correlation between  $F_{\varepsilon_\gamma > 100 \text{ MeV}}$  and the photon indices emerging from the power-law fits. Because no significant flux or spectral changes were observed during the pre- and post-flare epochs A (0–252 days) and C (294–374 days; see Figure 4), the average fluxes and photon indices for these time periods are reported. Note that the average fluxes of these pre- and post-flare epochs are comparable, whilst the corresponding photon indices differ significantly by  $\Delta\Gamma_\gamma \simeq 0.2$ . Moreover, the observed spectral evolution during one year of the *Fermi*-LAT exposure reveals a hysteresis-like character, more clearly seen for the flaring period (epoch B, with a time bin of 2 weeks), followed by a gradual flattening in the subsequent decay phase. Further insights into the spectral evolution of NGC 1275 within the *Fermi*-LAT photon energy range are provided by Figure 6, which shows the two SEDs for pre- and post-flare epochs A and C. Here, the dotted line corresponds to the best

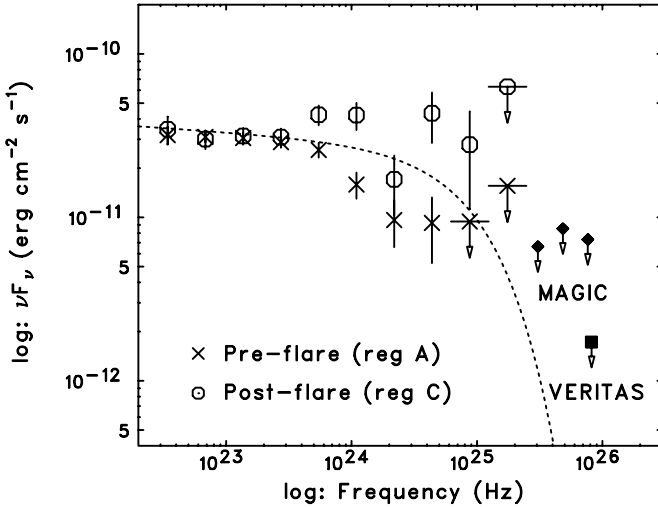


**Figure 6.**  $\gamma$ -ray SED of NGC 1275 before (crosses) and after the flare (open circles), corresponding to epochs A and C in Figure 4, respectively. Note that the excess high-energy  $\gamma$ -ray emission only appears above  $\varepsilon_\gamma \simeq 1\text{--}2$  GeV. The flux upper limits in the TeV range resulting from the VERITAS and MAGIC observations correspond to the pre-flare epoch A. The dotted line represents the best-fit cutoff power-law fit as given in Figure 3.

“power-law with an exponential cutoff” fit function determined from an average  $\gamma$ -ray spectrum, as given in Figure 3. Interestingly, the difference between the two SEDs consists of an excess at photon energies  $\varepsilon_\gamma \simeq 1\text{--}2$  GeV, with the low-energy  $\gamma$ -ray flux remaining essentially unchanged between the two epochs. This implies that (1) the  $\gamma$ -ray variability in NGC 1275 (and possibly other radio galaxies) may be restricted to  $\geq$  GeV photon energies, and that (2) the position of the peak in the high-energy spectral component (in the  $\nu F_\nu$  representation) may change substantially even within the same object with no accompanying significant flux changes. Note in this context that both the VERITAS and MAGIC non-detections were obtained during the pre-flare epoch A (164–206 days; see Acciari et al. 2009b; Aleksić et al. 2010). Hence, the emerging conclusion is that *it is not the total flux above 100 MeV which should play a major role in triggering TeV observations of steep-spectrum *Fermi*-LAT sources, but instead it is the flux and photon index determined at higher photon energies ( $\geq$  GeV).*

On the theoretical side, this conclusion could be possibly justified by noting that after a new episode of injection of freshly accelerated electrons into the emission zone (e.g., a downstream region of a shock), higher energy electrons may lag behind the lower-energy electrons. In such a case, as discussed previously in the context of blazar modeling (e.g., Kirk et al. 1998; Sato et al. 2008), a “counterclockwise” hysteresis in the flux versus photon index plane may arise, similar to what we observed in NGC 1275 at  $\gamma$ -ray photon energies.

Here, we comment on the question if NGC 1275—being a representative example of a low-power radio galaxy—may be considered as a misaligned blazar, most likely of the LBL type. Assuming a homogeneous jet model, one should expect its jet Doppler factor  $\delta = \Gamma_j^{-1}(1 - \beta_j \cos \theta)^{-1} = \Gamma_j^{-1}(1 - \sqrt{1 - \Gamma_j^{-2}} \cos \theta)^{-1} \simeq 1\text{--}2$ , for the typically expected jet viewing angle of  $\theta \simeq 20^\circ - 30^\circ$  and jet bulk Lorentz factors  $\Gamma_j \simeq 10$ . Indeed, modeling of the broadband emission of LBLs (beamed counterparts of radio galaxies such as NGC 1275 by assumption) requires  $\delta \sim \Gamma_j \sim 10$ . Thus, if the only difference

between radio galaxies and blazars is due to the viewing angle, this should manifest in (1) different observed positions of the spectral peaks in the  $\nu F_\nu$  representation ( $\nu \propto \delta$ ), (2) different observed variability patterns ( $t_{\text{var}} \propto \delta^{-1}$ , assuming the emission region is a moving source), and finally in (3) different observed luminosities ( $L_{\text{obs}} \propto \delta^4$  for a moving blob case, or  $\propto \delta^3/\Gamma_j$  for the steady jet; see Sikora et al. 1997).

Indeed, both the low- and high-energy  $\nu F_\nu$  peaks of NGC 1275 are located at substantially lower frequencies than those of typical LBLs. Taking the difference of beaming factors into account (i.e.,  $\delta_{\theta=0}/\delta_{\theta=20^\circ} \sim 10$ ), the broadband SED of the NGC 1275 would be similar to the SEDs of blazars such as BL Lacertae or 3C 66A. Note however that the position of the high-energy spectral peak may change substantially in a single object even for comparable flux levels, at least in NGC 1275, so the diagnostics related to the location of the spectral peaks may not be very conclusive.

Variability as short as day timescales is often observed in LBLs. For example, during the historical flare of BL Lacertae in 1997, correlated  $\gamma$ -ray and optical flares were observed, with the  $\gamma$ -ray flux increasing by a factor of 2.5 within a day (Bloom et al. 1997). Similarly, daily variability has been discovered in both *Fermi*-LAT and VERITAS observations of 3C 66A (Reyes et al. 2009). Hence, in the simple unification scheme outlined above, we should expect NGC 1275 to vary in  $\gamma$ -rays on timescales of several days. This, however, is difficult to test even with the excellent sensitivity of the *Fermi*-LAT instrument, due to the limited photon statistics for weekly time bins. The analysis presented in this paper gives instead only a robust upper limit  $t_{\text{var}} \leqslant$  a few months. However, note that day-timescale variability has been detected at TeV photon energy range for the M 87 radio galaxy (Acciari et al. 2009c). Thus, more frequent monitoring of NGC 1275 by ground-based Cherenkov telescopes would be valuable in this respect.

The observed photon flux of  $F_{\varepsilon_\gamma > 100\text{MeV}} = (2.19 \pm 0.13) \times 10^{-7}$  photons  $\text{cm}^{-2} \text{s}^{-1}$  implies an *observed* (isotropic)  $\gamma$ -ray luminosity of NGC 1275,  $L_\gamma \simeq 4\pi d_L^2 (\Gamma_\gamma - 1) F_{\varepsilon_\gamma > \varepsilon_0} \int_{\varepsilon_0}^{\varepsilon_c} (\varepsilon/\varepsilon_0)^{1-\Gamma_\gamma} d\varepsilon \sim 10^{44}$  erg  $\text{s}^{-1}$ , for  $\Gamma_\gamma \simeq 2.0\text{--}2.2$  and  $\varepsilon_c \simeq 42$  GeV. This is already comparable to the typical observed  $\gamma$ -ray luminosities of LBLs, which range between  $L_\gamma \sim 10^{44}$  and  $10^{46}$  erg  $\text{s}^{-1}$ . Note in particular that in the framework of the simple unification scheme discussed above, the beamed analog of NGC 1275 would then be characterized by the observed  $\gamma$ -ray luminosity larger by a factor of  $[\delta_{\theta=0}/\delta_{\theta=20^\circ}]^4 \sim 3 \times 10^4$  (or at least  $[\delta_{\theta=0}/\delta_{\theta=20^\circ}]^3 \sim 3 \times 10^3$ ) than this, i.e.,  $L_\gamma > 10^{47}$  erg  $\text{s}^{-1}$ . Such luminosities are not expected for LBL-type blazars (see Abdo et al. 2010a). On the other hand, the observed  $\gamma$ -ray luminosity of NGC 1275 is not energetically problematic, since the total *emitted*  $\gamma$ -ray power in this source seems rather moderate *as long as the emitting plasma moves with highly relativistic bulk velocities*, namely,  $L_{\gamma, \text{em}} \simeq (\Omega_j/4\pi) L_\gamma \simeq L_\gamma/4\Gamma_j^2 < 10^{42}$  erg  $\text{s}^{-1}$  for  $\Gamma_j \sim 10$ , where  $\Omega_j \simeq \pi\theta_j^2$  is the solid angle defined by the jet opening angle  $\theta_j$ , for which we assumed  $\theta_j \sim 1/\Gamma_j$ . Such a relatively small emitted power would constitute less than 1% of the total kinetic power of the NGC 1275 jet, estimated by Dunn & Fabian (2004) to be roughly  $L_j \sim (0.3\text{--}1.3) \times 10^{44}$  erg  $\text{s}^{-1}$ . Yet the problem of an unexpectedly large observed  $\gamma$ -ray luminosity of the beamed analog of NGC 1275 remains, and poses a serious challenge to the simplest version of the AGN unification scheme. In this context, a viable explanation for this problem would be to postulate that the high-energy emission ob-

served from “misaligned” blazars such as NGC 1275 (or M 87) is dominated not by a jet “spine” characterized by large bulk Lorentz factors ( $\Gamma_j \sim 10$  as is the case in bona-fide blazars), but by the slower jet boundary layers ( $\Gamma_j \sim \text{few}$ ) as discussed by several authors (e.g., Celotti et al. 2001; Stawarz & Ostrowski 2002; Ghisellini et al. 2005). Alternatively, one may propose that the  $\gamma$ -ray emission observed from radio galaxies is not produced within the “proper” blazar emission zone, but at larger distances from the active center characterized by slower bulk velocities (say,  $\Gamma_j \simeq \text{few}$ ) of the emitting plasma. Yet another possibility may be that the inner jets in NGC 1275 (and also in similar objects) are in general intrinsically less relativistic than the ones in bona-fide blazars; this would be consistent with the conclusions of Lister & Marscher (1997), who argue that radio-loud AGN with nuclear jets characterized by  $\Gamma_j \geq 10$  must be rather rare among the general population. Whichever scenario is correct, the *Fermi* results seem to indicate that low-power radio galaxies are most likely not simple off-axis analogs of BL Lac objects in terms of their  $\gamma$ -ray properties.

The *Fermi*-LAT Collaboration acknowledges generous ongoing support from a number of agencies and institutes that have supported both the development and the operation of the LAT as well as scientific data analysis. These include the National Aeronautics and Space Administration and the Department of Energy in the United States, the Commissariat à l’Energie Atomique and the Centre National de la Recherche Scientifique/Institut National de Physique Nucléaire et de Physique des Particules in France, the Agenzia Spaziale Italiana and the Istituto Nazionale di Fisica Nucleare in Italy, the Ministry of Education, Culture, Sports, Science and Technology (MEXT), High Energy Accelerator Research Organization (KEK), and Japan Aerospace Exploration Agency (JAXA) in Japan, and the K. A. Wallenberg Foundation, the Swedish Research Council, and the Swedish National Space Board in Sweden.

Additional support for science analysis during the operations phase is gratefully acknowledged from the Istituto Nazionale di Astrofisica in Italy and the Centre National d’Études Spatiales in France.

We acknowledge S. Digel and J. Finke for their helpful comments to improve the manuscript. Ł.S. is grateful for the support from the Polish MNiSW through the grant N-N203-380336.

## REFERENCES

- Abdo, A., et al. 2009a, *ApJ*, **699**, 31 (Paper I)
- Abdo, A., et al. 2009b, *ApJ*, **700**, 597 (LAT Bright AGN Sample)
- Abdo, A., et al. 2009c, *ApJS*, **183**, 46 (LAT Bright Source List)
- Abdo, A., et al. 2009d, *ApJ*, **707**, 55 (M87)
- Abdo, A., et al. 2010a, *ApJ*, **715**, 429
- Abdo, A., et al. 2010b, *ApJS*, submitted (arXiv:1002.2280v1)
- Acciari, V. A., et al. 2008, *ApJ*, **684**, L73
- Acciari, V. A., et al. 2009a, *ApJ*, **693**, L104
- Acciari, V. A., et al. 2009b, *ApJ*, **706**, L275
- Acciari, V. A., et al. 2009c, *Science*, **325**, 444
- Acciari, V. A., et al. 2009d, *ApJ*, **707**, 612
- Ajello, M., et al. 2009, *ApJ*, **690**, 367
- Albert, J., et al. 2007, *ApJ*, **666**, L17
- Aleksić, J., et al. 2010, *ApJ*, **710**, 634
- Anderhub, H., et al. 2009, *ApJ*, **704**, L129
- Asada, K., et al. 2006, *PASJ*, **58**, 261
- Atwood, W. B., et al. (*Fermi*-LAT Collaboration) 2009, *ApJ*, **697**, 1071
- Balmaverde, B., Capetti, A., & Grandi, P. 2006, *A&A*, **451**, 35
- Bloom, S. D., et al. 1997, *ApJ*, **490**, L145
- Böhringer, H., et al. 1993, *MNRAS*, **264**, L25
- Celotti, A., Ghisellini, G., & Chiaberge, M. 2001, *MNRAS*, **321**, L1
- Dunn, R. J. H., & Fabian, A. C. 2004, *MNRAS*, **355**, 862
- Fabian, A. C., et al. 2003, *MNRAS*, **344**, L43
- Fabian, A. C., et al. 2006, *MNRAS*, **366**, 417
- Ghisellini, G., Celotti, A., Fossati, G., Maraschi, L., & Comastri, A. 1998, *MNRAS*, **301**, 451
- Ghisellini, G., Tavecchio, F., & Chiaberge, M. 2005, *A&A*, **432**, 401
- Kirk, J. G., Rieger, F. M., & Mastichiadis, A. 1998, *A&A*, **333**, 452
- Lister, M. L., & Marscher, A. P. 1997, *ApJ*, **476**, 572
- Mayer-Hasselwander, H. A., et al. 1982, *A&A*, **105**, 164
- Owen, F. N., Eilek, J. A., & Kassim, N. E. 2000, *ApJ*, **543**, 611
- Reimer, O., Pohl, M., Sreekumar, P., & Mattox, J. R. 2003, *ApJ*, **588**, 155
- Reyes, L. C., et al. 2009, in Proc. 31st ICRC (arXiv:0907.5175)
- Sato, R., et al. 2008, *ApJ*, **680**, L9
- Sikora, M., Madejski, G., Moderski, R., & Poutanen, J. 1997, *ApJ*, **484**, 108
- Stawarz, Ł., & Ostrowski, M. 2002, *ApJ*, **578**, 763
- Strong, A. W., et al. 1982, *A&A*, **115**, 404
- Taylor, G. B., & Vermeulen, R. C. 1996, *ApJ*, **457**, L69
- Vermeulen, R. C., Readhead, A. C. S., & Backer, D. C. 1994, *ApJ*, **430**, L41
- Walker, R. C., et al. 2000, *ApJ*, **530**, 233
- Weekes, T. C., et al. 2002, *Astropart. Phys.*, **17**, 22